Digital Total Variation filtering as postprocessing for Radial Basis Function Approximation Methods

Scott A. Sarra
Marshall University

February 26, 2006

Abstract

Digital total variation (DTV) filtering techniques, that originated in the field of image processing, are adapted to postprocess Radial Basis Function approximations of piecewise continuous functions. Through numerical examples, we show that DTV filtering is a fast, robust, postprocessing method that can be used to remove Gibbs oscillations while sharply resolving discontinuities. The method is applicable for arbitrarily located data points. A postprocessing method for scattered data had not been given previously.

keywords: Gibbs phenomena, Radial Basis Functions, meshfree, Digital Total Variation filtering, postprocessing.

1 Introduction

Over the last several decades radial basis functions (RBFs) have been found to be successful for the interpolation of smooth functions on scattered data sets. More recently, the RBF methods have emerged as an important type of method for the numerical solution of partial differential equations (PDEs) [1, 2]. Most PDE results have concerned steady state problems with smooth solutions. Recently there has been a growing interest in applying RBF methods to time-dependent PDE problems, again to problems with sufficiently smooth solutions.

Like most approximation methods and particularly global methods, the accuracy of the RBF methods is severely degraded by Gibbs oscillations when the underlying function is only piecewise continuous. Many physical phenomenon are represented by piecewise smooth functions. However, this

does not rule out the accurate modelling of these phenomenon by methods which are plagued by the Gibbs phenomenon. Often a very accurate approximation can be recovered from the initial oscillatory approximation via a postprocessing technique.

For the more developed pseudospectral method [3], there are several postprocessing methods [4], the most powerful of which require the knowledge of the exact location of the discontinuities. The process of pinpointing the exact location of the discontinuities is in itself a challenging problem. The difficulty of edge detection is increased when discontinuities are not aligned with a cartesian grid and/or when the data is scattered in irregularly shaped domains. Typically, postprocessing methods that do not incorporate edge detection are easier to apply but inferior in accuracy to methods that do.

Recently Digital Total Variation (DTV) filtering, which is based on image processing ideas, has been presented as a postprocessing method for Chebyshev pseudospectral approximations to conservation laws [5]. The DTV filter was shown to be a fast, robust, postprocessing method for accelerating the convergence of pseudospectral approximations that have been contaminated by Gibbs oscillations. The DTV filter sharply resolves discontinuities without prior knowledge of edge locations as it has built-in edge detection. Unlike other pseudospectral postprocessing methods, the DTV filter does not require that the data be located on a structured pseudospectral grid. Thus, it is a more general method.

To date, there have been few applications of RBF methods to problems with discontinuities or even very steep gradients. In one dimension, adaptive methods for problems with step gradients have been proposed [6, 7], but problems with shocks or other discontinuities have not been effectively dealt with. The stability of RBF methods for conservation laws has yet to be addressed. Postprocessing methods for scattered RBF approximations of piecewise continuous functions have not been described.

In this work we discuss the application, with some modifications, of the DTV filter to scattered approximations by radial basis functions.

2 RBF interpolation

A *radial basis function* $\phi(r)$ is a continuous univariate function that has been radialized by composition with the Euclidean norm on $\mathbb{R}^d$. Globally supported RBFs may or may not have a free parameter called the *shape parameter* which we denote by c. Well known RBFs without a shape pa-

Name of RBF	Definition
Multiquadric (MQ)	$\phi(r,c) = \sqrt{1 + c^2 r^2}$
Inverse Quadratic (IQ)	$\phi(r,c) = 1/(1 + c^2 r^2)$
Gaussian (GA)	$\phi(r,c) = e^{-c^2 r^2}$
Matern (MT)	$\phi_\nu(r,c) = \frac{2^{1-\nu}}{\Gamma(\nu)}(cr)^\nu K_\nu(cr)$

Table 1: Global, infinitely smooth RBFs

rameter are the *polyharmonic splines*

$$\phi(r) = \begin{cases} r^{2k-d} & \text{if } 2k-d > 0 \text{ is an odd integer} \\ r^{2k-d} \log r & \text{if } 2k-d > 0 \text{ is an even integer.} \end{cases} \tag{1}$$

This class of RBF typically approximates smooth functions with algebraic convergence rates. Some commonly used RBFs which are infinitely differentiable and have a shape parameter are listed in table 1. In the definition of the Matern RBF, K_v is a modified Bessel function and $\nu > 0$ is a smoothness parameter. This class can exhibit spectral rates of convergence in approximating smooth functions. The interested reader is referred to the recent book by Buhmann [8] for more basic details about RBFs.

Let Ξ be a finite distinct set of points in $\mathbb{R}^d$, which are traditionally called *centers* in the language of RBFs. The RBF interpolant consists of a RBF expansion and augmented polynomials

$$s(x) = \sum_{i=0}^{N} \gamma_i \phi(\|x - \xi_i\|_2) + \sum_{j=0}^{m-1} \tau_j p_j(x), \quad x \in \mathbb{R}^d \tag{2}$$

where $\{p_j(x)\}_{j=0}^{m-1}$ is a basis for space, Π_{m-1}^d, of algebraic $d-$variate polynomials that are of degree less than or equal to $m-1$. The additional degrees of freedom are taken up by requiring that

$$\sum_{i=0}^{N} \gamma_i p_j(x_i) = 0, \quad j = 0, \dots, m-1. \tag{3}$$

If ϕ is positive definite ($m = 0$), as in the case of the IQ and GA, the the un-augmented RBF interpolation problem is uniquely solvable. If ϕ is only conditionally positive definite (CPD) of order $m > 0$, polynomial terms must be added to the RBF expansion [9]. The polyharmonic splines are conditionally positive definite of order $m = k - \lfloor d/2 \rfloor + 1$. For more

information on CPD functions see [8]. The MQ is CPD of order $m = 1$ but the un-augmented interpolation problem is nonsingular because of special properties of the MQ [9].

The expansion coefficients, γ_i and τ_j, are found by requiring that

$$s|_\Xi = f|_\Xi \tag{4}$$

for given data $f|_\Xi$. That is, they are obtained by solving the linear system

$$H \begin{bmatrix} \gamma \\ \tau \end{bmatrix} = \begin{bmatrix} A & P \\ P^T & 0 \end{bmatrix} \begin{bmatrix} \gamma \\ \tau \end{bmatrix} = \begin{bmatrix} f|_\Xi \\ 0 \end{bmatrix} \tag{5}$$

where the elements of the matrix A are $A_{i,j} = \phi(\|\xi_i - \xi_j\|_2)$ for $i, j = 0, 1, \ldots, N$ and the elements of P are $P_{i,j} = p_j(x_i)$ for $i = 0, 1, \ldots, N$ and $j = 0, \ldots, m - 1$.

The conditioning of H is a practical concern. The interpolation matrix may be very ill-conditioned as the separation distance between centers decreases. For RBFs containing a shape parameter such as those in table 1, small shape parameters produce the most accurate results, but are also associated with a poorly conditioned interpolation matrix.

3 Digital TV filtering

Variational based PDE restoration methods, such as total variation (TV) filtering [10], have become one of the most important tools in image processing. These methods assume that the images are defined on a continuous domain and a continuous variational functional is constructed from which an Euler-Lagrange equation is derived. The resulting differential equations are then discretized by existing numerical PDE methods on a cartesian grid. Another approach is to *digitize* the entire methodology. This approach starts directly with a discrete variational problem and works with data on a general discrete domain, a graph. The digitized approach is more flexible as irregularly shaped domains and scattered data points can be handled with ease. Digital total variation (DTV) filtering, developed in [11] and further analyzed in [12], is one such digitized method. In the context of numerical PDEs, it has previously been applied to steady solutions of conservation laws computed by second-order Lax-Wendroff methods in [13] and [14] and to the numerical solution of conservation laws by pseudospectral methods in [5]. Next, the pertinent facts about the DTV filter from are summarized and the reader is referred to [11, 12] for details.

Let $[\Omega, G]$ be a finite set Ω of nodes and G a dictionary of edges. Vertices are denoted by $\alpha, \beta, \cdots$. The notation $\alpha \sim \beta$ indicates that α and β are linked by an edge. All the neighbors of α are denoted by

$$N_\alpha = \{\beta \in \Omega \,|\, \beta \sim \alpha\}. \tag{6}$$

We start with a set of function values u^0 on Ω that are contaminated by Gibbs oscillations. The oscillations are removed by solving an unconstrained minimization problem that minimizes a fitted TV energy. The solution of the minimization problem is a system of nonlinear equations which can be shown to have a unique solution that depends on a parameter λ and on u^0. The nonlinear system can be solved by a linearized Jacobi iteration as

$$u_\alpha^{[n+1]} = \sum_{\beta \sim \alpha} h_{\alpha\beta} u_\beta^{[n]} + h_{\alpha\alpha} u_\alpha^0. \tag{7}$$

The filter coefficients are defined by

$$h_{\alpha\beta}(u) = \frac{w_{\alpha\beta}(u)}{\lambda + \sum_{\gamma \sim \alpha} w_{\alpha\gamma}(u)} \tag{8}$$

and

$$h_{\alpha\alpha}(u) = \frac{\lambda}{\lambda + \sum_{\gamma \sim \alpha} w_{\alpha\gamma}(u)} \tag{9}$$

where

$$w_{\alpha\beta}(u) = \frac{1}{|\nabla_\alpha u|_a} + \frac{1}{|\nabla_\beta u|_a}. \tag{10}$$

The *regularized location variation* or strength at any node α is defined as

$$|\nabla_\alpha u|_a = \left[\sum_{\beta \in N_\alpha} (u_\beta - u_\alpha)^2 + a^2 \right]^{1/2}. \tag{11}$$

The parameter λ is a *fitting parameter* corresponding to a Lagrange multiplier in the variational problem that has been digitized. The *regularization parameter a* is a small constant to avoid a zero local variation and to ensure the stability of the algorithm. We have used $a = 10^{-8}$ in our numerical examples. The iteration can be initialized by setting $u^{[0]} = u^0$. After the first several iterations the corrections to the previous iteration are very small. An effective stopping criteria is for the relative L^1 residual between two consecutive iterations to be less than some tolerance, i.e.,

$$\frac{\left\| u^{[k+1]} - u^{[k]} \right\|_{L^1}}{\left\| u^{[k]} \right\|_{L^1}} \le tol. \tag{12}$$

An estimation of the optimal fitting parameter for a current signal $u^{[n]}$ is [11]

$$\lambda^{[n]} \approx \frac{1}{\sigma^2} \frac{1}{N+1} \sum_{\alpha \in \Omega} \sum_{\beta \sim \alpha} w_{\alpha\beta}(u_\beta^{[n]} - u_\alpha^{[n]})(u_\alpha^{[n]} - u_\alpha^0) \tag{13}$$

where σ^2 is the *variance of the noise*. The filtering process can be started with

$$\lambda = \frac{1}{\sigma^2}, \tag{14}$$

and then updated every several steps with (13). However, if the initial λ is used throughout the entire filtering process the results are typically just as good as if λ had been updated every several steps. A wide range of λ results in an accurate post-processing. Since the Gibbs oscillations are not random noise, a more effective way to specify the fitting parameter λ is based on the strength of the oscillations. More insight is provided in the numerical examples.

The digital TV filter is a lowpass filter since

$$h_{\alpha\alpha} + \sum_{\beta \in N_\alpha} h_{\alpha\beta} = 1, \quad \alpha \in \Omega. \tag{15}$$

Because of the lowpass filter property the digital TV filter satisfies the *maximum principle*

$$\min_\beta u_\beta^0 \le u_\alpha^{[n]} \le \max_\beta u_\beta^0 \tag{16}$$

at each node α. Unlike other post-processing algorithms, the DTV filter has built-in edge detection. For a properly chosen regularization constant λ, e.g. as specified by equation (14), a jump in the data will be indicated by the weights $w_{\alpha\beta}$ being small compared to λ. This in turn causes $h_{\alpha\alpha}$ to be near one which leads to a large portion of the original data being retained as the filter is applied. On the other hand, in smooth regions, the weights are large compared to λ, $h_{\alpha\beta}$ will be large and $h_{\alpha\alpha} \ll 1$ which leads to the oscillations in the data being smoothed.

4 DTV filtering as RBF postprocessing

To illustrate the properties of the DTV filtering we interpolate the step function

$$f(x) = \begin{cases} 1 & -1 \le x \le 0, \\ 0 & 0 < x \le 1 \end{cases} \tag{17}$$

known at N scattered centers to $M = 199$ points that cluster around the discontinuity at $x = 0$ and that are specified by $x_j = \frac{2}{\pi} \arcsin\left(\frac{-1+2j}{M-1}\right)$, $j = 0, \ldots, M - 1$. The results are shown for $N = 79$ in the left image of figure 1. For $N = 39, 79, 159$ the pointwise errors of the RBF approximation are in the left image of figure 2 and the errors of the DTV postprocessed step function approximations are shown in the right image of figure 1. The MQ RBF was used and for $N = 39, 79, 159$ the shape parameter and fitting parameter as ordered pairs (c, λ) were respectively $(1.8, 1)$, $(6, 1)$, and $(16, 15)$. This example provides some insight into the proper choice of the fitting parameter λ. A wide range of λ results in an accurate post-processing. However, the best results are attained with small λ for slowly oscillating functions, for example when $N = 39$ and $N = 79$, and larger λ for more rapidly oscillating functions, for example when $N = 159$. The acceleration of the convergence is impressive and the jump is sharply resolved. For each N, the postprocessing was completed in under one second. All numerical examples were executed on a 3.00 GHz pentium 4 processor with Windows XP using Matlab 6.5. Source code is available from the author by request. Additionally, the TV filtering algorithm will be available in the forthcoming updated version of [15] in the form of a Matlab toolbox.

There is a fundamental difference in the Gibbs oscillations in RBF approximations and in interpolating Chebyshev approximations to piecewise continuous functions. For $c > 0$, the Gibbs oscillations in RBF approximants are more localized. For RBF approximants, the order of the max norm errors are largely unaffected sufficiently away from a discontinuity, while for Chebyshev approximants the orders of the max norm errors are reduce to $1/N$. Near discontinuities, $\mathcal{O}(1)$ errors are present in both RBF and Chebyshev approximants. A comparison of RBF and Chebyshev approximations of function (17) is given in figure 2. In the limit as $c \to 0$, the RBF and interpolating Chebyshev interpolant are known to be identical [16] and intuitively we expect the the Gibbs oscillations in the two approximations to behave more similarly for smaller c than for larger values of the shape parameter.

In addition to postprocessing RBF interpolants, the DTV filter can be used to postprocess numerical PDE solutions by RBF methods. PDE solutions, particulary nonlinear hyperbolic conservation laws, have both sharp fronts and finely detailed features. The following function is used as an example:

$$f(x) = \begin{cases} 1.0 + e^{20(x-0.32)} & 0 \le x < 0.32, \\ 0.5 & 0.32 \le x \le 0.6, \\ 1.5 & 0.6 < x \le 1. \end{cases} \tag{18}$$

A desirable feature of a postprocessing method is that it removes oscillations and at the same time it sharply resolves fronts and does not smear fine features in the solution such as the spike near $x = 0.32$ in function (18). The left image of figure 3 shows the function and its oscillatory RBF approximation on a nonuniform grid selected by an adaptive grid algorithm [7]. The right image of figure 3 shows the DTV filter postprocessed approximation. In the postprocessed solution, the discontinuities are sharply resolved and the fine scale features are preserved.

5 Two-dimensional data

For two-dimensional scattered data, there are many ways to define N_α. One is to consider a p point neighborhood of a node α consisting of the p points that are closest to α. For arbitrary scattered data the flaw in this strategy is quickly exposed as it is possible for the points in the neighborhood to be configured as in the left image of figure 4 with all its members on one side of α. A more effective strategy is to divide the region surrounding a point α into p regions of equal angle and define N_α to consist of the points in each region that are closest to α. This strategy does not usually result in the p closest points to α but does ensure that N_α includes points in all directions around α. We have used $p = 8$ in all examples. An example neighborhood is shown in the right image of figure 4.

On the unit circle consider the function

$$f_1(x, y) = \begin{cases} 1 & x < 0 \\ 0 & x \geq 0. \end{cases} \tag{19}$$

The RBF approximation on the set of scattered points shown in the left image of figure 7 is displayed in the left image of figure 5 and the DTV postprocessed approximation is in the right image. The pointwise errors are shown in figure 6. The discontinuity is sharply resolved and the region of significant errors is reduced to a small neighborhood of the discontinuity.

Consider a function with a more complicated discontinuity structure

$$f_2(x, y) = \begin{cases} 2 & x, y < 0 \text{ and } |x| + |y| \geq 1, \\ 1 & x \geq 0 \text{ and } y < 0 \text{ or,} \\ & x < 0 \text{ and } y \geq 0 \\ 0 & x, y > 0 \text{ and } x^2 + y^2 < 0.5, \end{cases} \tag{20}$$

on the domain outlined in the right image of figure 7. A contour plot of function (20) is in figure 8. The MQ RBF approximation on the set of

scattered points in the right image of figure 7 is shown in the left image of figure 9. The DTV postprocessed approximation is in the right image of figure 9. For piecewise constant functions in two dimensions, even on widely scattered centers, the DTV filter is just as effective as it is for all functions in one dimension.

For piecewise continuous, but not piecewise constant functions on widely scattered centers the standard application of the DTV filter is not as successful. For very smooth regions the underlying function can be represented by a relatively sparse coverage of points. Between the sparsely located points the change in function values may be large enough for the DTV algorithm to mistake them as Gibbs oscillations unless the knowledge about the distance between the centers is incorporated into the algorithm. Figure 11 shows an idealized situation with two function values u_α and v_α and their respective closest neighboring function values u_β and v_β. Assuming a appropriate distribution of centers, the large jump in the u data over a small distance indicates a steep front near u_α while the large jump in the v data over a large distance should be recognized as a region of smoothness.

As an example consider the function

$$f_3(x, y) = \begin{cases} e^{-x/8} & x \leq 0 \\ 0 & x > 0 \end{cases} \tag{21}$$

approximated (left image of figure 10) by the RBF $\phi(r) = r^3$ on the scattered set of points on the unit circle shown in the left image of figure 7. In the smooth but non-constant region of $(x < 0, y)$ the points are sparsely scattered and are clustered around the discontinuity at $(x = 0, y)$. Applying the standard DTV filter results in the postprocessed approximation in the left image of figure 12. In the smooth region with sparely scattered centers the large variation in function values between points is mistaken as noise and the smooth region is distorted. Next we discuss two remedies.

5.1 Modifications

5.1.1 weighted graphs

If the centers are not too widely scattered using a weighted graph can improve the postprocessing. This approach introduces a weight function W to allow more influence in the filtering process from the points in N_α closest to α and less influence from the more distant points in N_α. Equation (11)

is modified to include the influence of the weight

$$\|\nabla_g u_\alpha\|_a = \left[\sum_{\beta \in N_\alpha} (u_\beta - u_\alpha)^2 W_{\alpha,\beta} + a^2 \right]^{1/2} \tag{22}$$

where W is a real positive weight function. A possible weight function is

$$W_{\alpha,\beta} = \left(\frac{\max_{\beta \in N_\alpha} dist(\alpha,\beta)}{dist(\alpha,\beta)} \right)^4.$$

5.1.2 indicator functions

Another approach is to introduce an indicator function

$$\eta(\alpha) = \max_{\beta \in N_\alpha} \frac{|u_\alpha - u_\beta|}{dist(\alpha,\beta)} \tag{23}$$

which measures the maximum ratio of jumps in function values to the distance between corresponding points over a neighborhood N_α. If $\eta(\alpha)$ is greater than a prescribed tolerance the DTV filter is activated at α and otherwise it is not. The indicator function for the cubic RBF approximation of the function in equation (21) is displayed in the right image of figure 10. The use of the indicator function results in the postprocessed approximation in the right image of figure 12. Applying the DTV filter only in select regions results in a good postprocessed approximation. This is largely due to the previous comments about the local nature of the Gibbs oscillations in RBF approximations. In our numerical experiments, the indicator function method was always superior to the weighted graph approach.

6 Conclusions

The DTV filter has been presented as a method to remove Gibbs oscillations from global RBF approximations of discontinuous functions. The oscillatory approximants could arise from a interpolation problem or from a numerical PDE problem. Without the need for separate edge detection methods, the DTV filter sharply resolves discontinuities and improves the overall accuracy of an oscillatory RBF approximation in a robust, computationally efficient manner. Numerical examples show the effectiveness of DTV filtering for scattered RBF approximations.

Issues that arise in RBF approximations with scattered nodes that are not present in structured pseudospectral approximations have been identified. An effective choice of a neighborhood, N_α, in two dimensions was identified. The use of an indicator function η was shown to be effective in selecting which points in a widely scattered data set receive postprocessing.

A fundamental difference between Gibbs oscillations in pseudospectral and RBF methods was identified. The oscillations in RBF approximations of discontinuous functions are more localized than those in pseudospectral approximants.

References

[1] E. Kansa. Multiquadrics - a scattered data approximation scheme with applications to computational fluid dynamics I: Solutions to parabolic, hyperbolic, and elliptic partial differential equations. *Computers and Mathematics with Applications*, 19(8/9):147–161, 1990.

[2] E. Kansa. Multiquadrics - a scattered data approximation scheme with applications to computational fluid dynamics I: Surface approximations and partial derivative estimates. *Computers and Mathematics with Applications*, 19(8/9):127–145, 1990.

[3] Claudio Canuto, M. Y. Hussaini, Alfio Quarteroni, and Thomas A. Zang. *Spectral Methods for Fluid Dynamics*. Springer-Verlag, New York, 1988.

[4] D. Gottlieb and J. Hesthaven. Spectral methods for hyperbolic problems. *Journal of Computational and Applied Mathematics*, pages 83–131, 2001.

[5] S. A. Sarra. Digital total variation filtering as postprocessing for Chebyshev pseudospectral methods for conservation laws. *To appear in Numerical Algorithms*, 2006.

[6] Y. Hon and X. Mao. An efficient numerical scheme for Burger's equation. *Appl. Math. Comput.*, pages 37–50, 1998.

[7] S. A. Sarra. Adaptive radial basis function methods for time dependent partial differential equations. *Applied Numerical Mathematics*, 54(1):79–94, 2005.

[8] M. D. Buhmann. *Radial Basis Functions*. Cambridge University Press, 2003.

[9] C. Micchelli. Interpolation of scattered data: Distance matrices and conditionally positive definite functions. *Constructive Approximation*, 2:11–22, 1986.

[10] A. Fatemi L. Rudin, S. Osher. In *Proceedings of the 11th annual international conference of the Center for Nonlinear Studies on Experimental mathematics*, pages 259–268, 1992.

[11] T. Chan, S. Osher, and J. Shen. The digital TV filter and nonlinear denoising. *IEEE Transactions on Image Processing*, 10(2), 2001.

[12] S. Osher and J. Shen. Digitized PDE method for data restoration. In G. Anastassiou, editor, *Analytic-Computational Methods in Applied Mathematics*, chapter 16, pages 751–771. Chapman and Hall/CRC, 2000.

[13] A. Burgel, T. Grahs, and T. Sonar. From continuous recovery to discrete filtering in numerical approximations of conservation laws. *Applied Numerical Mathematics*, 42:47–60, 2002.

[14] A. Burgel and T. Sonar. Discrete filtering of numerical solutions to hyperbolic conservation laws. *International Journal for Numerical Methods in Fluids*, 40:263–271, 2002.

[15] S. A. Sarra. The spectral signal processing suite. *ACM Transactions on Mathematical Software*, 29(2), 2003. www.scottsarra.org/signal/signal.html.

[16] T. Driscoll and B. Fornberg. Interpolation in the limit of increasingly flat radial basis functions. *Computers and Mathematics with Applications*, 43:413–422, 2002.
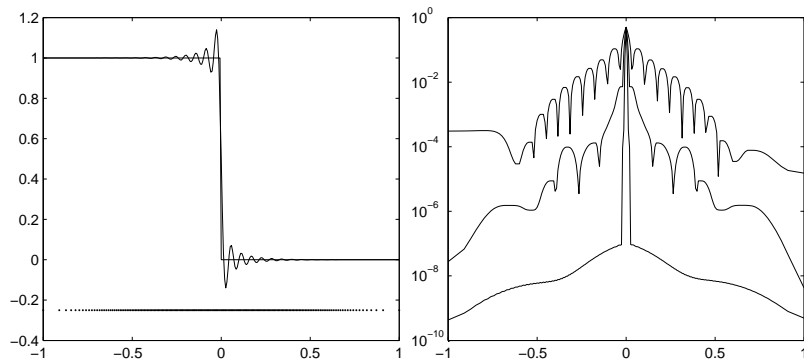
Figure 1: Left: $N = 79$ RBF approximation (oscillatory) of function (17) vs. exact on grid indicated by dots at the bottom of the image. Right: Convergence of DTV post-processed RBF approximation of function (17). From top to bottom, $N = 39, 79, 159$.
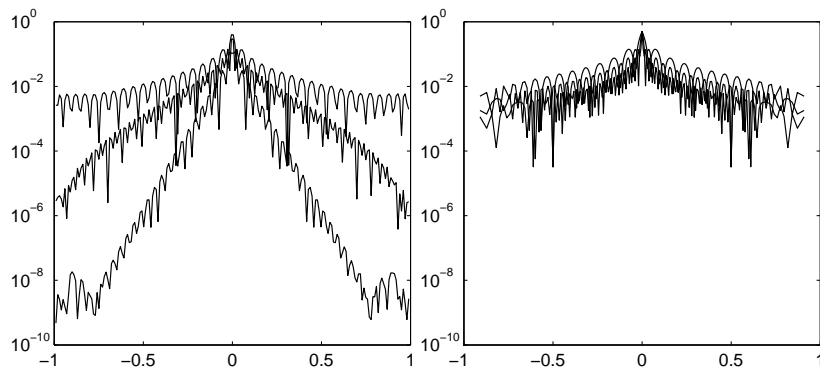

Figure 2: Left: Convergence of RBF approximation of function 17. From top to bottom, $N = 39, 79, 159$. Right: Chebyshev approximation of function 17, $N = 39, 79, 159$

13
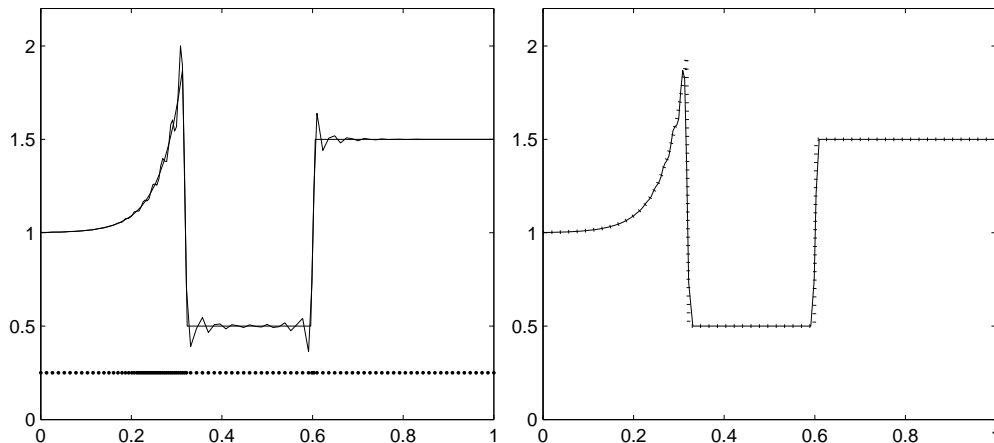
Figure 3: Left: RBF approximation (oscillatory) using the MQ RBF with $c = 15$ vs. exact on the $N = 100$ grid indicated by dots at the bottom of the image. Right: Exact (dotted) vs. postprocessed (solid) RBF approximation of function (18) with $\lambda = 15$ after 100 iterations taking 0.03 second.
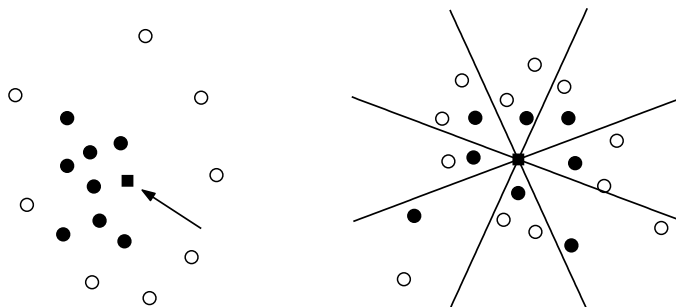
Figure 4: Left: A neighborhood N_α (filled circles) resulting from choosing the eight closest points to α. Such a neighborhood can result in a poor postprocessing due to points clustering on one side of α. Right: Eight point neighborhood N_α of the point α (the square in the center) chosen by selecting the closest point to α in each of eight regions. Filled circles are in N_α, open circles are not.

14
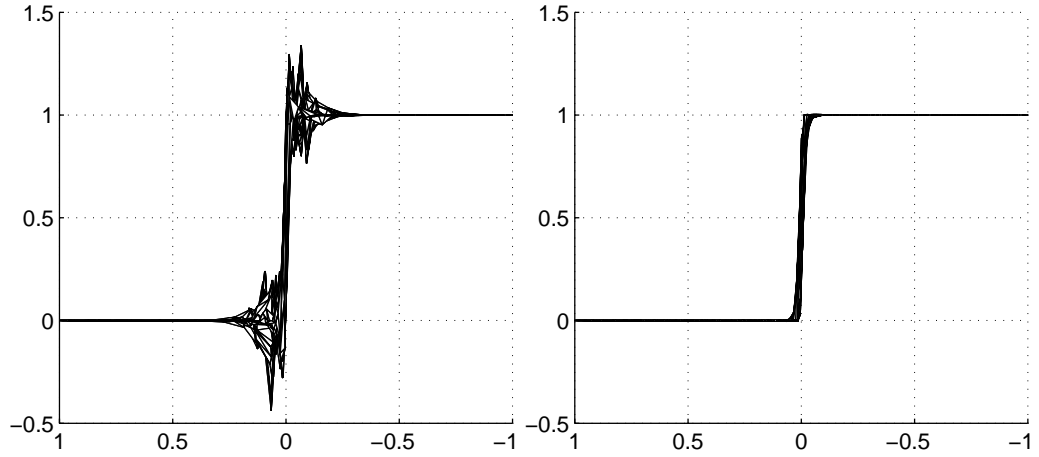
Figure 5: Left: From viewpoint $(180, 0)$ the MQ RBF approximant with $c = 18$ on scattered points (left image of figure 7). Right: DTV postprocessed with $\lambda = 12$ after 40 iterations taking 3 second.
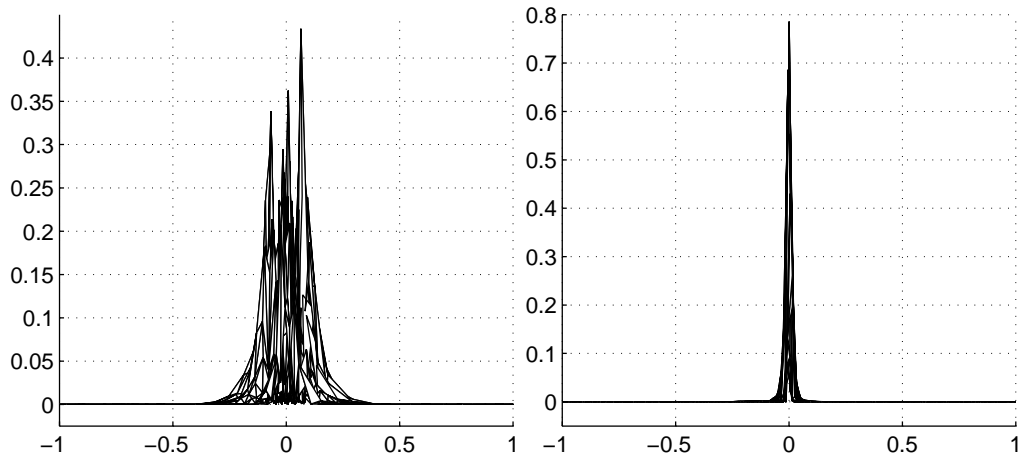
Figure 6: From viewpoint $(-0.5, 6)$, absolute value of errors from figure 5 approximants. Left: RBF. Right: Postprocessed RBF
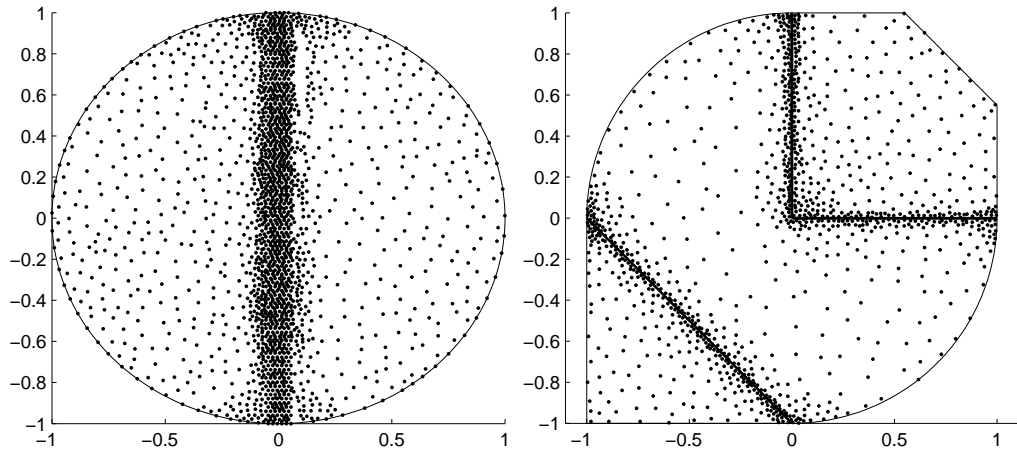
Figure 7: Left: $N = 2047$ scattered points on the unit circle. Right: $N = 1126$ scattered points on a complexly shaped domain.
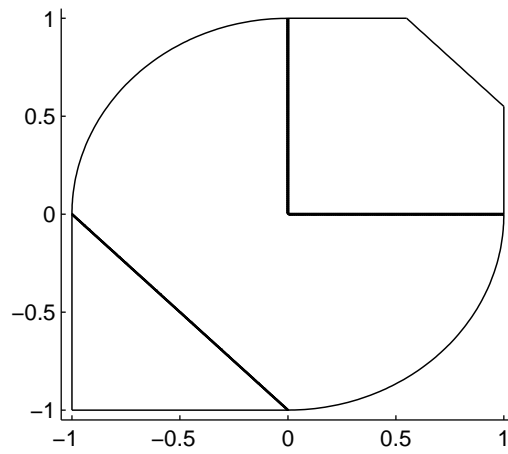

Figure 8: Contour plot of function 20.

16
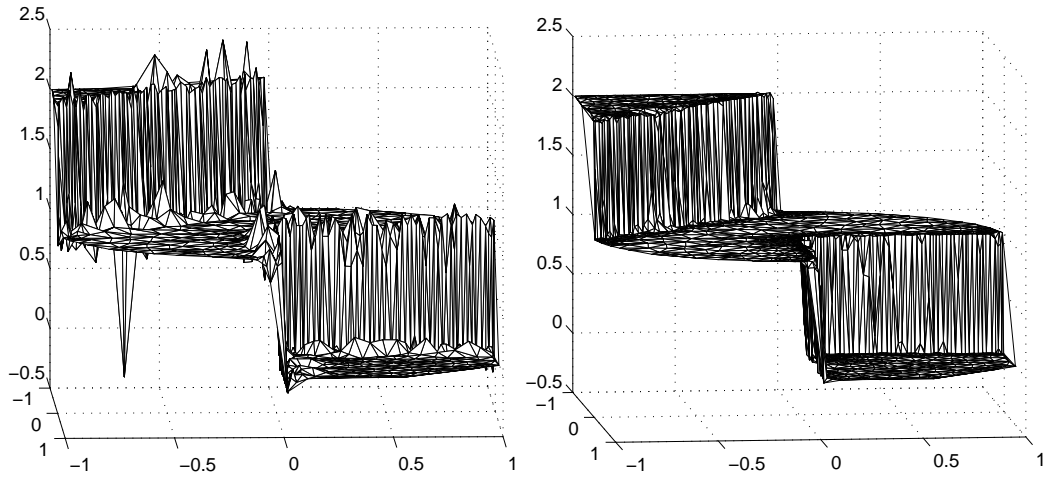
Figure 9: Left: MQ RBF approximation, $c = 18$, of function 20 (on scattered points from left image of figure 7). Right: DTV postprocessed with $\lambda = 25$ after 50 iterations.
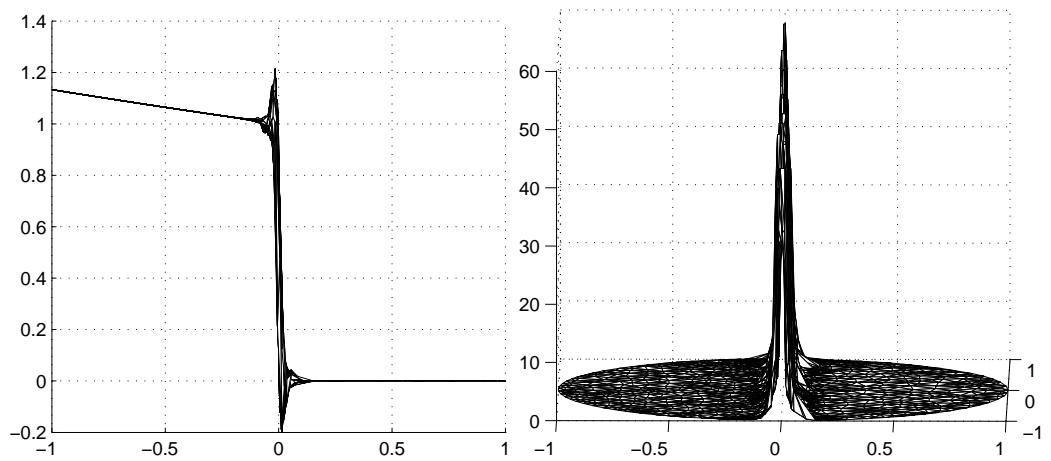

Figure 10: Left: $\phi(r) = r^3$ approximation of function (21) on the distribution of points in the left image of figure 7. Right: Indicator function (23) for the approximation in the left image.
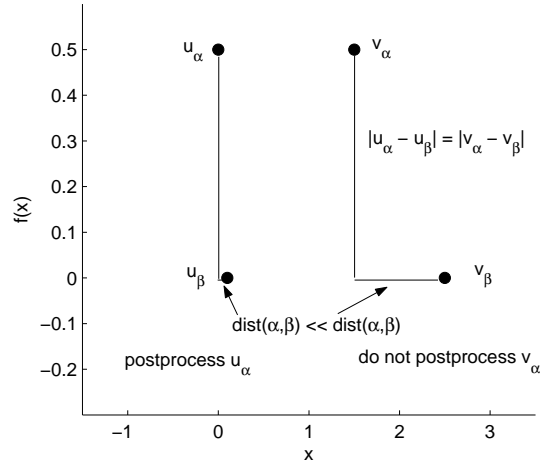
Figure 11: The indicator function causes DTV postprocessing to be applied at u_α but not at v_α.
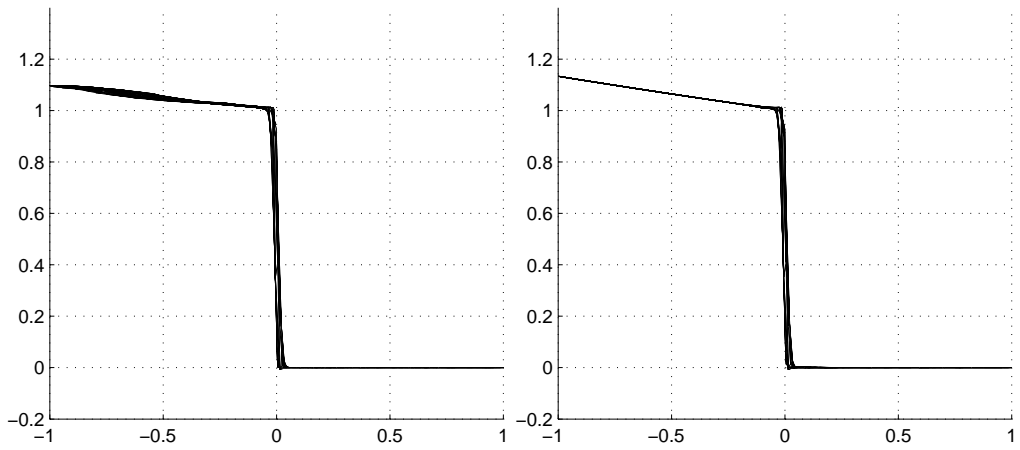

Figure 12: Left: Standard DTV filtering, five iterations with $\lambda = 18$. Right: DTV filtering activated where the indicator function is greater than 0.2.